Conformational Behavior and Magnetic Properties of Organic Radicals Derived from Amino Acid Residues. The Dipeptide Analogue of Glycine Radical

Vincenzo Barone,*,† Carlo Adamo,‡ Andre Grand,§ Yvon Brunel,⁺ Marc Fontecave,⁺ and Robert Subra⁺

Contribution from the Dipartimento di Chimica, Università Federico II, via Mezzocannone 4, I-80134 Napoli, Italy, Dipartimento di Chimica, Università della Basilicata, via Nazario Sauro 85, I-85100 Potenza, Italy, Service d'Etudes des Systemes et Architectures Moleculaires (SESAM), DRFMC, CEN Grenoble, BP 85X, F-38041-Grenoble Cedex, France, and Laboratoire d'Etudes Dynamiques et Structurales de la Selectivite (LEDSS), Universite Joseph Fourier, 301 Avenue de la Chimie, BP 53X, F-38041 Grenoble Cedex, France

Received May 16, 1994[⊗]

Abstract: A general quantum mechanical protocol for the study of flexible open-shell systems has been applied to a simple model of the glycine radical engaged in peptide chains. The conformational freedom of the resulting dipeptide analogue is severely restricted with respect to that of standard amino acid residues. Only planar or quasi-planar conformations are energetically accessible due to π-electron delocalization on the whole compound. As a consequence, the structural parameters and the vibrational frequencies involving the C^{α} atom are typical of ethylenic systems. The hyperfine coupling constants of the $C^{\alpha}H$ moiety remain, however, similar to those of the prototype methyl radical and show the same strong dependence on out-of-plane deformations. The hyperfine coupling constants of the NH moiety are, instead, only dependent on the backbone conformation. Vibrationally averaged hyperfine coupling constants both of $C^{\alpha}H$ and NH moieties are in fair agreement with experimental values of glycine radicals produced in some proteins.

Introduction

The importance of protein radicals has been appreciated only recently. While such species were first viewed as degradation products during reactions with harmful OH radicals, or upon exposure to irradiation,[1−3] it was found that enzymes may specifically utilize radicals on intrinsic amino acid residues as cofactors. Such a strategy allows a fine one-electron gating mechanism, in which a single redox equivalent can be stored and then processed at a time. The prototype of such radical enzymes is the aerobic ribonucleotide reductase and its tyrosyl radical.[4]

Glycine radicals,[5] formed during activation of two anaerobic enzymes (pyruvate formate lyase, PFL,[6] and ribonucleotide reductase, RNR[7]) have been identified very recently, and are not as well characterized as tyrosyl radicals in terms of geometrical structure, electron density, magnetic properties, and reactivity. In particular, it is interesting to understand why the same glycine radical gives rise to different EPR signals and how these are modulated by different environments. This is the kind of analysis where theory can play its most profitable role. Only in a theoretical framework, in fact, can different terms be selectively switched on and off, to analyze general trends, or to verify different hypotheses. Of course, the computational level must be sufficient to describe, in a balanced way, the interactions governing the physico-chemical properties of interest. In the present context this involves at the same time noncovalent interactions and magnetic properties.

The quantitative reproduction of hydrogen bond strengths requires large, multiply polarized basis sets and proper account of correlation effects.[8,9] This level of computation is out of question for biological molecules, but we have recently shown that Hartree−Fock computations with polarized double ζ basis sets are remarkably accurate concerning both structural and energetic aspects.[10] This is to be ascribed, of course, to some error compensation (essentially between basis set superposition error and lack of correlation energy) but, from a pragmatic point of view, offers a viable computational model. The more so, as recent studies[11] have shown that the same level of computation

† Università Federico II.
‡ Università della Basilicata.
§ Service d'Etudes des Systemes et Architectures Moleculaires.
⁺ Universite Joseph Fourier.
⊗ Abstract published in *Advance ACS Abstracts,* December 15, 1994.

(1) Neta, P.; Fessenden, R. W. *J. Phys. Chem.* **1971**, *75*, 738−748.
(2) Hayon, E.; Ibata, T.; Lichtin, N. N.; Simic, M. *J. Am. Chem. Soc.* **1971**, *93*, 5388−5394.
(3) Livingston, R.; Doherty, D. G.; Zelders, H. *J. Am. Chem. Soc.* **1975**, *97*, 3198−3204.
(4) (a) Reichard, P.; Ehrenberg, A. *Science* **1983**, *221*, 514−519. (b) Sahlin, M.; Petersson, L. Gräslund, A.; Ehrenberg, A.; Sjöberg, M.; Thelander, L. *Biochemistry* **1987**, *26*, 5541−5548. (c) Bender, C.; Sahlin, M.; Babcock, G. T.; Barry, B. A.; Chandrasekhar, T. K.; Salowe, S. P.; Stubbe, J.; Lindstrom, B.; Petersson, L.; Ehrenberg, A.; Sjoberg, B. M. *J. Am. Chem. Soc.* **1989**, *111*, 8079−8083. (d) DeGray, J. A.; Lassmann, G.; Curtis, J. F.; Kennedy, T. A.; Marnett, L. A.; Eling, T. E.; Mason, R. P. *J. Biol. Chem.* **1992**, *267*, 23 583−235 88. (e) Babcock, G. T.; El-Deeb, M. K.; Sandusky, P. O.; Whittaker, M. M.; Whittaker, J. W. *J. Am. Chem. Soc.* **1992**, *114*, 3727−3734. (f) Hoganson, C. W.; Babcock, G. T. *Biochemistry* **1992**, *31*, 11874−11880.
(5) (a) Hayon, E.; Simic, M. *J. Am. Chem. Soc.* **1971**, *93*, 6781−6786. (b) Kirino, Y.; Taniguchi, H. *J. Am. Chem. Soc.* **1976**, *98*, 5089−5096.
(6) Volker, V.; Wagner, A. F.; Frey, M.; Neugerbauer, F. A.; Knappe, J. *Proc. Natl. Acad. U.S.A.* **1992**, *89*, 996−1000.
(7) Mulliez, E.; Fontecave, M.; Gaillard, J.; Reichard, P. *J. Biol. Chem.* **1993**, *268*, 2296−2299.
(8) Szalewicz, K.; Cole, S. J.; Kolos, W.; Barlett, R. J. *J. Chem. Phys.* **1988**, *89*, 3662−3671.
(9) Latajaka, Z. *THEOCHEM* **1991**, *251*, 245−260.
(10) Amodeo, P.; Barone, V. *J. Am. Chem. Soc.* **1992**, *114*, 9085−9093.
(11) Barone, V.; Cristinziano, P. L. *Chem. Phys. Lett.* **1993**, *215*, 40−44.

0002-7863/95/1517-1083$09.00/0

provides an accurate description of the conformational behavior of saturated and aromatic systems not involving hydrogen bridges.

At the same time, the hyperfine coupling constants of free radicals provide a severe challenge to theoretical chemistry, since they are related to subtle details of the ground state electronic wave function. This has stimulated much work, and the most sophisticated post-Hartree−Fock (especially coupled clusters[12,13] or multireference configuration interaction[14−16]) and density functional (including gradient corrections[17−19]) models are providing wave functions of sufficient quality. However, the first class of methods is too expensive for systematic studies of large molecules, and the second class is still not sufficiently tested. Recent studies have shown that, at least for carbon centered π and quasi-π radicals, wave functions obtained by low order perturbative correlation treatments give expectation values of the spin density at nuclei close to those obtained by more sophisticated approaches.[12,20,21] Furthermore, the same polarized double ζ basis set introduced for conformational studies seems quite adequate also for the study of magnetic properties.[12,20] Although this would define, in principle, a viable strategy for electronic computations, the reliability of hyperfine couplings obtained at this level has been recently questioned.[14] We have, therefore, performed some test computations with larger basis sets and more complete inclusion of correlation energy for a number of small model systems.

From another point of view, vibrational averaging of the hyperfine coupling constants by large amplitude inversion motions at the radical center can sometimes be very important; for instance, the isotropic hyperfine splitting of ^{13}C in methyl radical is enhanced by about 30% by vibrational averaging.[20] We have recently shown that the combined use of correlated electronic wave functions with medium size basis sets and proper account of vibrational modulation effects through effective large amplitude nuclear Hamiltonians provide a powerful and reliable tool to investigate EPR features of flexible radicals.[20,22] Here we apply this general quantum mechanical protocol to a comprehensive study of the conformational behavior and magnetic properties of glycine radical. Some comment is, however, in order about the model systems selected in the present paper. In fact, any theoretical study involves a certain degree of idealization. The significance of the loss of information connected with such a process requires constant confrontation with experiment. In particular, both short- and long-range interactions play significant roles in peptides and proteins. Local effects can be investigated by models as simple as the so-called dipeptide analogues.[10,23] This is the topic of the present paper. Investigation of the balance between intra- and inter-residue interactions requires much larger systems[10] and will be dealt with in future studies by means of molecular modeling.

Computational Methods

Electronic computations have been performed with the GAUSSIAN 92[24] and ACES/2[25] codes and the vibrational studies by the DiNa package.[22,26] Electronic wave functions were generated by the unrestricted (UHF) formalism, correlation energy being then introduced by many-body perturbation theory employing the Moller−Plesset Hamiltonian partitioning[27] carried to second order (UMP2) or by the coupled cluster approach including single and double excitations and a perturbative estimate of triples (UCCSD[T])[28]. All electrons were always correlated. Although the wave function consisting of UHF orbital does not represent a correct spin state, all the computations reported in the present study give $0.75 < S^2 < 0.78$, and annihilation of the quartet contribution leaves essentially no residual spin contamination ($S^2 < 0.751$). In such circumstances we can expect good structures and spin dependent properties from unrestricted computations.

A full double-ζ polarized basis set is the smallest reasonable set for determination of hyperfine parameters, since each highly occupied orbital requires a partner spin polarization orbital that is localized in roughly the same region of space, but is typically a little more diffuse. Although not all double-ζ and larger bases provide satisfactory results, one that does is Dunning's [42/2] contraction of the Huzinaga (9s,5p/4s) basis.[29a] When augmented by single polarization functions on all atoms,[29b] this basis set, hereafter referred to as HD, has been our standard for the computation of spin-dependent properties. As mentioned in the Introduction, the same basis set performs very well also in structural and conformational problems. Some test computations have been also performed by the (10,6,1;5,1)/[6,4,1:3,1] basis set introduced by Chipman[30] and further validated in ref 20b (referred to as TZP$^+$ basis set).

The structures of the most significant conformers have been fully optimized by gradient methods at the UHF/HD level. More reliable energy differences and spin-dependent properties have been obtained by single point UMP2/HD computations at the above geometries. The formulas for calculating hyperfine parameters are obtained from the spin Hamiltonian[31]

$$H_{spin} = -g\beta S_z B_z - g_N \beta_N I_z B_z + SAI$$

(12) (a) Sekino, H.; Bartlett, R. J. *J. Chem. Phys.* **1985**, *82*, 4225−4229. (b) Pereira, S. A.; Watts, J. D.; Bartlett, R. J. *J. Chem. Phys.* **1994**, *100*, 1425−1434.

(13) Carmichael, I. *J. Phys. Chem.* **1991**, *95*, 6198−6201.

(14) Feller, D.; Glendening, E. D.; McCullough, E. A., Jr.; Miller, R. J. *J. Chem. Phys.* **1993**, *99*, 2829−2840.

(15) Fernández, B.; Jøogensen, P.; McCullough, E. A., Jr.; Symons, J. *J. Chem. Phys.* **1993**, *99*, 5995−6003.

(16) (a) Engels, B. *J. Chem. Phys.* **1994**, *100*, 1380−1386. (b) Suter, H. U.; Engels, B. *J. Chem. Phys.* **1994**, *100*, 2936−2942.

(17) (a) Barone, V.; Adamo, C.; Russo, N. *Chem. Phys. Lett.* **1993**, *212*, 5−11. (b) Barone, V.; Adamo, C.; Russo, N. *Int. J. Quantum Chem.* **1994**, *52*, 963−971. (c) Adamo, C.; Barone, V.; Fortunelli, A. *J. Phys. Chem.* **1994**, *98*, 8648−8652.

(18) (a) Eriksson, L. A.; Malkin, V. G.; Malkina, O. L.; Salahub, D. R. *J. Chem. Phys.* **1993**, *99*, 9756−9763. (b) Kong, J.; Eriksson, L. A.; Boyd, R. J. *Chem. Phys. Lett.* **1993**, *217*, 24−30. (c) Eriksson, L. A.; Malkina, O. L.; Malkin, V. G.; Salahub, D. *J. Chem. Phys.* **1994**, *100*, 5066−5075. (d) Austen, M. A.; Eriksson, L. A.; Boyd, R. J. *Can. J. Chem.* **1994**, *72*, 695−704.

(19) (a) Barone, V. *Chem. Phys. Lett.* **1994**, *226*, 392−398. (b) Barone, V. *J. Chem. Phys.* **1994**, *101*, 6834−6838. (c) Barone, V.; Adamo, C.; Fortunelli, A. *J. Chem. Phys.* **1995**, in press.

(20) (a) Barone, V.; Minichino, C.; Faucher, H.; Subra, R.; Grand, A. *Chem. Phys. Lett.* **1993**, *205*, 324−330. (b) Barone, V.; Minichino, C.; Grand, A.; Subra, R. *J. Chem. Phys.* **1993**, *99*, 6787−6798. (c) Barone, V.; Grand, A.; Minichino, C.; Subra, R. *J. Phys. Chem.* **1993**, *97*, 6355−6361.

(21) Cramer, C. J. *J. Am. Chem. Soc.* **1991**, *113*, 2439−2447. (b) Cramer, C. J. *Chem. Phys. Lett.* **1993**, *202*, 297−302. (c) Cramer, C. J., Lim, M. H. *J. Phys. Chem.* **1994**, *98*, 5024−5033.

(22) (a) Minichino, C.; Barone, V. *J. Chem. Phys.* **1994**, *100*, 3717−3741. (b) Barone, V.; Minichino, C. *THEOCHEM*, in press.

(23) Barone, V.; Fraternali, F.; Cristinziano, P. L. *Macromolecules* **1990**, *23*, 2038−2044.

(24) Frisch, M. J.; Trucks, G. W.; Head-Gordon, M.; Gill, P. M. W.; Wong, M. W.; Foresman, J. B.; Johnson, B. G.; Schlegel, H. B.; Robb, M. A.; Replogle, E. S.; Gomperts, R.; Andres, J. L.; Raghavachari, K.; Binkley, J. S.; Gonzalez, C.; Martin, R. L.; Fox, D. J.; DeFrees, D. J.; Baker, J.; Stewart, J. J. P.; Pople, J. A. GAUSSIAN92; Gaussian Inc., Pittsburgh, PA, 1992.

(25) Stanton, J. F.; Gauss, J.; Watts, J. D.; Lauderdale, W. J.; Bartlett, R. J. *Int. J. Quantum Chem., Chem. Symp.* **1992**, *26*, 879−894.

(26) Barone, V.; Jensen, P.; Minichino, C. *J. Mol. Spectrosc.* **1992**, *154*, 252−264.

(27) Moller, C.; Plesset, M. S. *Phys. Rev.* **1934**, *46*, 618−622.

(28) (a) Bartlett, R. J.; Watts, J. D.; Kucharski, S. A.; Noga, J. *Chem. Phys. Lett.* **1990**, *165*, 513−522. (b) Rittby, M.; Bartlett, R. J. *J. Phys. Chem.* **1988**, *92*, 3033−3036. (c) Watts, J. D.; Gauss, J.; Bartlett, R. J. *Chem. Phys. Lett.* **1992**, *200*, 1−7.

(29) (a) Dunning, T. H., Jr. *J. Chem. Phys.* **1970**, *53*, 2823. (b) Dunning, T. H., Jr.; Hay, P. J. In *Modern Theoretical Chemistry*; Schaefer, H. F., III, Ed.; Plenum Press: New York, 1977; Vol. 2, Chapter 1.

(30) Chipman, D. M. *Theor. Chim. Acta* **1989**, *76*, 73−84; *J. Chem. Phys.* **1989**, *91*, 5455−5465.

The first two contributions are the electronic and nuclear Zeeman terms, respectively, and arise from the interactions between a magnetic field B and the magnetic moments of the unpaired electrons (S_z) or the magnetic nuclei (I_z) in the system. The remainder is the hyperfine interaction term, and is a result of the interactions between the unpaired electrons and the nuclei. β_e, β_N are the electron and nuclear magnetons, and g_N is the nuclear magnetogyric ratio.

The 3 × 3 hyperfine interaction tensor A can be further separated into its isotropic (spherically symmetric) and anisotropic (dipolar) components. Isotropic hyperfine splittings a_N in MHz are related to the spin densities $\varrho^s(\mathbf{r}_N)$ at the corresponding nuclei by

$$a_N = \frac{8\pi}{3}\beta_e g_N \beta_N \sum_{\mu,\nu} P^{\alpha\text{-}\beta}_{\mu,\nu} \langle \varphi_\mu | \delta(\mathbf{r}_{kN}) | \varphi_\nu \rangle$$

Computation of these terms is straightforward and is already included in most ab initio codes.

The anisotropic components are derived from the classical expression of interacting dipoles:

$$T_{i,j}^{(N)} = \beta_e g_N \beta_N \sum_{\mu,\nu} P^{\alpha\text{-}\beta}_{\mu,\nu} \langle \varphi_\mu | r_{kN}^{-5} (r_{kN}^2 \delta_{ij} - 3 r_{kN,i} r_{k,N,j}) | \varphi_\nu \rangle$$

These terms are more complicated to compute, and also to determine experimentally. They are, however, strictly related to field-gradient integrals already available in several standard ab inition packages.

For planar radicals (assumed to lie in the xy plane), it is interesting to consider the components of the hyperfine tensor parallel ($A_{||}$) or prependicular ($A_\perp$) to the molecular plane. They are given by:

$$A_{||} = a + {}^1/_2(T_{xx} + T_{yy}) = a - {}^1/_2\, T_{zz} \text{ and } A_\perp = a + T_{zz}$$

The splittings are usually given in units of MHz by microwave spectroscopists and in gauss (1 G = 0.1 mT) by EPR spectroscopists. In the present work all the values are given in gauss and, assuming that the free electron g value is appropriate also for the radicals. To convert data to MHz, one has to multiply by 2.8025.

The study of large amplitude vibrations requires, especially in the case of large molecules, some separation between the active large amplitude (LA) motion and the *spectator* small amplitude (SA) ones. If the LAM occurs along the steepest descendent path in the mass weighted coordinate space (the so called intrinsic large amplitude path, ILAP[32]),, the gradient is parallel to the path so that first order potential couplings between LAM and SAM's disappear.[33] For intramolecular dynamics, however, the simpler distinguished coordinate (DC) approach has the advantage of being invariant upon isotopic substitutions and also well defined beyond energy minima. This model corresponds to the construction of the one-dimensional path through the optimization of all the other geometrical parameters at selected values of a specific internal coordinate.

When the ILAP is traced, successive points are obtained following the energy gradient. Because there is no external force or torque, the path is nonrotational and leaves the center of mass fixed.[33] Successive points coming from separate geometry optimizations (as is the case for the DC model) introduce the additional problem of their relative orientation. In fact, the distance in mass weighted Cartesian coordinates between adjacent points is altered by the rotation or translation of their respective reference axes. The problem of translations has the trivial solution for centering the reference axes at the center of mass of the system. On the other hand, for nonplanar systems, the problem of rotations does not have an analytical solution and must be solved by numerical minimization of the distance between successive points as a function of the Euler angles of the system.[34]

(31) Weltner, W., Jr. *Magnetic Atoms and Molecules*; Van Nostrand: New York, 1983.
(32) Fukui, K. *J. Phys. Chem.* **1970**, *74*, 4161−5163; *Acc. Chem. Res.* **1981**, *14*, 363−368.
(33) Miller, W. H.; Handy, N. C.; Adams, J. E. *J. Chem. Phys.* **1980**, *72*, 99−112.
(34) Zhixing, C. *Theor. Chim. Acta* **1989**, *75*, 481−483.

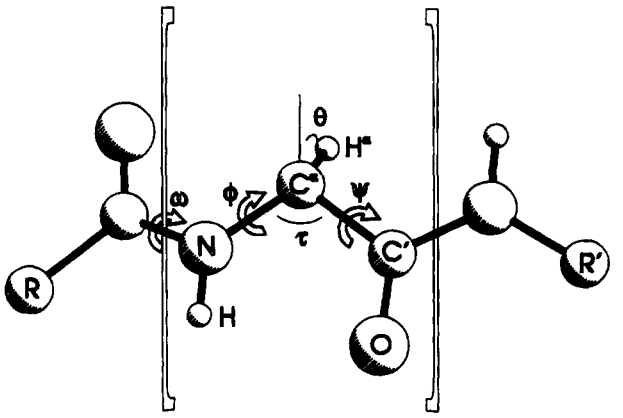

Figure 1. Atom labeling and principal geometrical parameters of glycine radical engaged in peptidic chains.

When the coupling terms are negligible, the adiabatic Hamiltonian governing the motion along the large amplitude path assumes the simple form:

$$H(s,\boldsymbol{n}) = {}^1/_2 p_f^2 + V_{ad}(s,\boldsymbol{n})$$

where

$$V_{ad}(s,\boldsymbol{n}) = V_0(s) - V_0(s^0) + \hbar \sum_{i=1}^{f-1} (n_i + {}^1/_2)(\omega_i(s) - \omega_i(s^0))$$

$\omega_i(s)$'s are the harmonic frequencies of SA vibrations as a function of the large amplitude coordinate, and s^0 refers to a suitable reference structure lying on the path. The adiabatic potential obtained when all the corresponding quantum numbers are 0 is usually referred to as ground state vibrationally adiabatic potential ($V_{gs}(s)$). If, further, the vibrational frequencies of SAM's do not vary very much along the path, the motion along the LAP is governed by the bare potential $V_0(s)$.

The successive step consists in determining vibrational eigenvalues and eigenfunctions. Local basis set methods are tailored to this end since they give reliable results independently of the shape of the profile. Cubic splines were used to interpolate the potential along the LAP and to generate a larger set of equispaced points on which cubic splines were used as basis functions.[35] The expectation value $\langle O \rangle_j$ of a given observable in the vibrational eigenstate $|j>$corresponding to the eigenvalue ϵ_j is given by:

$$\langle O \rangle_j = O_{\text{ref}} + \langle j(s) | \Delta O(s) | j(s) \rangle$$

where O_{ref} is the value of the observable at the reference configuration, and $\Delta O(s)$ is the expression (here a spline fit) giving its variation as a function of the progress variable s. The temperature dependence of the observable is obtained by assuming a Boltzmann population of the vibrational levels, so that:

$$\langle O \rangle_T = O_{\text{ref}} + \frac{\sum_{j=0}^{\infty} \langle j | \Delta O | j \rangle \exp[(\epsilon_0 - \epsilon j)/KT]}{\sum_{j=0}^{\infty} \exp([\epsilon_0 - \epsilon_j)/KT]}$$

Results and Discussion

(a) Conformational Behavior. In order to investigate the possible conformations of the glycine radical in protein structures, we have considered the model F−GlyR−NH_2, where F stands for formyl group, and GlyR for −HN−CH−CO (Figure 1). The model for the parent molecule is F−Gly−NH_2, where

(35) Cremaschi, P. *Mol. Phys.* **1980**, *40*, 401−409.

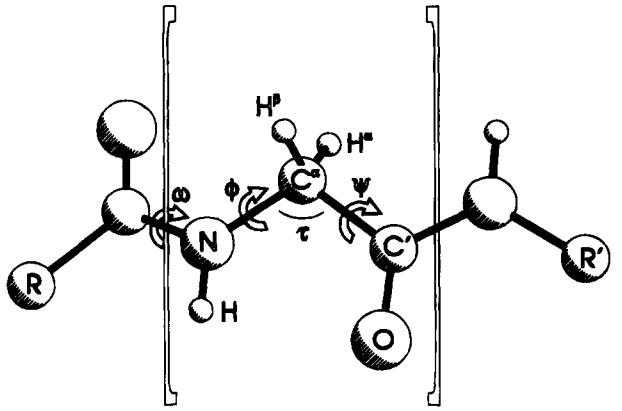

Figure 2. Atom labeling and principal geometrical parameters of a glycine residue engaged in peptidic chains.

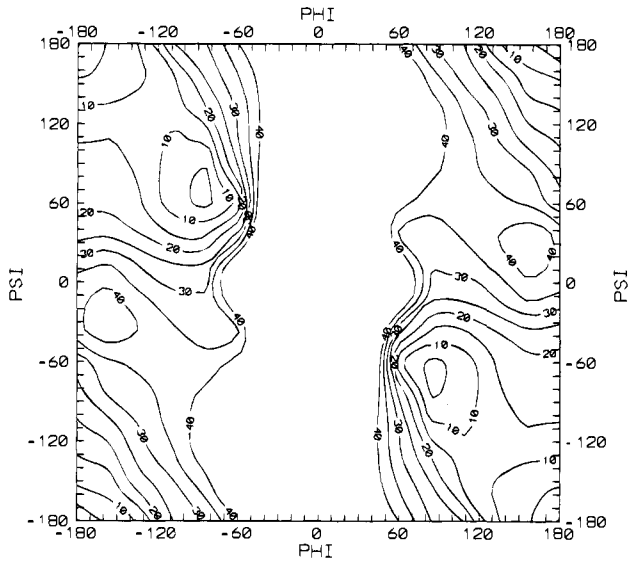

Figure 3. Rigid rotor (ϕ, ψ) map of F−Gly−NH_2 obtained by HF/HD computations. Contour lines are drawn every 5 kJ mol^{-1} up to 40 kJ mol^{-1} above the absolute minimum.

Gly stands for −HN−CH_2−CO (Figure 2). The adequacy of formyl and NH_2 terminal groups in place of the more usual acetyl and $NHCH_3$ moieties has been tested in previous studies.[10,23]

Regular structures are classified in terms of the number of atoms forming the "cycle" closed by an H-bond between NH and OC groups belonging to the backbone. According to this scheme, the extended conformation typical of β-sheets is labeled C_5 ($\phi \approx 180°$, $\psi \approx 180°$); γ turns are labeled C_7 ($\phi \approx 90°$, $\psi \approx -60°$); α-helices and their "variations", which differ in the exact number of residues per turn (from 3.7 in an ideal α-helix up to 4) are labeled C_{13} ($\phi \approx 60°$, $\psi \approx 30°$). Standard labels[14] are, instead, used for semiextended structures, namely, α′ for $\phi = 180°$, $\psi = 60°$, P_{II} for $\phi = 60°$, $\psi = 180°$, and β for the so-called bridge structure ($\phi \approx 90°$, $\psi \approx 0°$).

A first validation of our computational procedure has been obtained through a complete UHF/HD geometry optimization of the C_5 conformation of F−Gly−NH_2 (see Table 1). Using this geometry, a rigid rotor (RR) Ramachandran (ϕ, ψ) map has been built (Figure 3). If an upper limit of 20−25 kJ mol^{-1} is used to define allowed conformations, the conformational freedom of this residue is essentially restricted to the region limited by C_5 and bridge structures, and including the C_7 conformer. Two nearly isoenergetic minima are found in that region, corresponding to the C_5 and C_7 conformers. The map shows a third local minimum ($\phi \approx 160°$, $\psi \approx 30°$), roughly

Table 1. UHF/HD Geometrical Parameters for the C_5 Conformation of F−Gly−NH_2 and for the C_5 and α′ Conformations of F−GlyR−NH_2[a]

parameter	F−Gly−NH_2 (C_5 conf)	F−GlyR−NH_2 (C_5 conf)	F−Gly−Nh_2 (α′ conf)
C^{α}-N	1.437	1.379	1.390
N-Cf	1.345	1.362	1.368
Cf-Of	1.201	1.215	1.193
Cf-Hf	1.091	1.080	1.090
N-H	0.996	1.002	0.998
C^{α}-Cμ	1.520	1.445	1.453
C′-N′	1.352	1.357	1.391
N′-Hc	0.995	0.995	0.998
N′-Ht	0.996	0.996	0.998
C′-O	1.203	1.234	1.201
C^{α}-H^{α}	1.086	1.066	1.069
C^{α}NCf	121.5	123.2	122.8
NCfOf	124.6	123.8	124.7
CfHf	113.0	113.0	112.4
CfNH	121.2	121.5	117.6
C^{α}C′N′	114.8	116.9	116.7
C′N′Hc	122.2	122.8	115.7
C′N′Ht	118.4	118.5	112.0
N′C′O	123.0	122.8	122.2
C^{α}NCfOf	0.0	0.0	−6.6
C^{α}NCfHf	180.0	180.0	173.9
OfCfNH	180.0	180.0	−173.8
C^{α}C′N′Hc	0.0	0.0	−43.8
C^{α}C′N′Ht	180.0	180.0	−174.5
HcN′C′O	180.0	180.0	139.2
τ	109.3	116.1	121.4
θ		0.0	0.1
ϕ	180.0	180.0	172.1
ψ	180.0	180.0	−10.5

[a] Hf, Cf, and Of are the atoms of the terminal formyl group; N′, Hc, and Ht are the atoms of the terminal NH_2 group (H$_t$ being trans to C^{α}), and the labeling of other atoms is standard (see Figure 1). Bond lengths are in Å and angles in degrees.

corresponding to the α′ structure, about 40 kJ mol^{-1} above the absolute energy minimum. The standard α helical conformation does not correspond to a local energy minimum, lies about 35 kJ mol^{-1} above the absolute minimum, and is less stable than the bridge structure. Despite the crudeness of the RR model, these results are in nice agreement with experimental findings for small peptides not perturbed by environmental effects.[36,37] Larger models must be considered to study the onset of helical structures characteristic of proteins.[10,23] For instance, at least three residues (besides terminal groups) are necessary to form the hydrogen bridge stabilizing α-helices.

The same general procedure has been followed to investigate the conformational freedom of F−GlyR−NH_2. The optimized geometry of the C_5 conformer is given in Table 1, and the Ramachandran map in Figure 4. The most striking difference between Figures 3 and 4 is the strong reduction of conformational freedom for glycine radical with respect to the parent molecule. In particular only planar or nearly planar conformations are now allowed, whereas the C_7 minimum is completely disappeared. Although this result would seem inconsistent with the reduction of steric hindrance related to elimination of one H^{α} atom, it becomes prefectly reasonable when considering the modification of the electronic structure. As a matter of fact, replacement of an sp^3 C^{α} atom by an sp^2 one allows an effective electron delocalization along the whole structure. This induces, in turn, a greater resistence to deformations destroying the planarity of the system. This effect is well evidenced by the structural parameters of Table 1. In fact, the most striking

(36) Yamazaki, T.; Abe, A. *Biopolymers* **1988**, *27*, 969−984.
(37) Grenie, Y.; Avignon, M.; Garrigou-Lagrange, C. *J. Mol. Struct.* **1974**, *24*, 293−307.

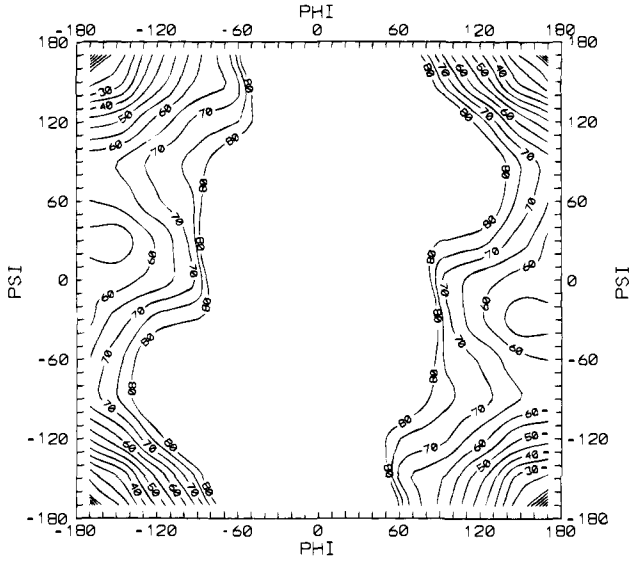

Figure 4. Rigid rotor (ϕ, ψ) map of F−GlyR−NH_2 obtained by HF/HD computations. Contour lines are drawn every 5 kJ mol^{-1} up to 80 kJ mol^{-1} above the absolute minimum.

differences between radical and parent molecule concern the local environment of the C^α atom: the $NC^\alpha C'$ angle is much larger in the radical, and the NC^α,$C^\alpha C'$ bond lengths quite shorter. Other minor geometry modifications are also consistent with the extension of the π-system on the whole radical, whereas the CH_2 moiety of the parent molecule inhibits conjugation between the F−NH and CO−NH_2 terminal groups. The α' minimum is present also for F−GlyR−NH_2, but ϕ and ψ angles have opposite signs ($\approx-170°$,20° or $\approx170°$,−20°), whereas they have the same sign in the parent molecule F−Gly−NH_2 ($\approx160°$,30° or $\approx-160°$,−30°). The nature of this conformer has been verified by full geometry optimization and computation of the harmonic force field. It corresponds to a true local minimum (all the computed frequencies are real) lying 15 kJ mol^{-1} above the C_5 minimum. Single point MP2 computations at UHF geometries increase the energy difference between C_5 and α' structures to 29 kJ mol^{-1}.

As a whole, our results show that GlyR is a very rigid residue, whose conformational characteristics cannot be described by empirical force fields optimized for standard residues. This does not allow the study of the onset of helical structures in larger models until a purposely tailored force field is built from the present ab initio result. The energy difference between helical and extended structures in F−GlyR−NH_2 (75 kJ mol^{-1}) is, however, more than double the corresponding figure in F−Gly−NH_2. This strongly suggests that the GlyR residue retains an extended or nearly extended conformation even when incorporated in helical motifs.

(b) EPR Parameters. As a first step, we considered it important to further validate our computational model (concerning both basis set and level of correlation) by performing some benchmark computations on a simple model retaining the essential features of the radical center in GlyR. To this end we have chosen the NH_2CH_2 radical.[1] Although the equilibrium structure of this system is strongly pyramidal,[38] we consider here a hypothetical planar structure, which more closely resembles the situation encountered in GlyR. The isotropic hyperfine splittings (hfs) computed by different methods are shown in Table 2. It is quite apparent that the UMP2/HD results are quite reliable for hydrogen atoms. On the other hand, the effect of basis set extension is negligible for carbon, whereas proper inclusion of correlation is quite significant. Just the opposite situation is found for nitrogens. Since the contemporary inclusion of both enhancements is prohibitive for larger systems, we will stay at the UMP2/HD level, which provides, anyway, semiquantitative results, the more so as only hydrogen atoms are unequivocally detected in the EPR experiments (vide infra), and those are well reproduced at this level of theory.

(38) Barone, V. *Chem. Phys. Lett.*, in press.

Table 2. Isotropic Hyperfine Splittings (Gauss) Obtained by Different Methods for the Planar Structure of the NH_2CH_2 Radical[a]

atom	UCCSD[T]/TZP+	UCCSD[T]/HD	UMP2/TZP+	UMP2/HD
^{13}C	22.1	23.9	17.6	18.1
^{14}N	1.9	2.7	1.9	2.9
H(C)	−22.1	−25.6	−21.1	−24.4
H(N)	−7.8	−8.9	−7.7	−9.0

[a] The geometry has been optimized at the UMP2/HD level.

Table 3. Isotropic Hyperfine Splittings (Gauss) of Different Atoms in F−GlyR−NH_2 Obtained by the UMP2/HD Computations at UHF/HD Geometries

atom	a ($\alpha = 0°$)	$\langle\Delta a\rangle_0$	$\langle\Delta a\rangle_1$	$\langle\Delta a\rangle_{298}$	$\langle a\rangle_{298}$	$\langle a'\rangle^a$
	C_5, D(UHF) = −375.226 09 au, E(UMP2) = −376.368 57 au, ν = 534 cm^{-1}					
C^α	12.8	3.0	8.2	3.4	16.2	19.0
H^α	−19.5	0.8	2.2	0.9	−18.6	−16.8
N	0.6	0.0	0.1	0.0	0.6	0.4
H_N	−5.6	0.3	0.7	0.3	−5.3	−4.6
	a', ΔE(UHF) = 15.0 kJ mol^{-1}, ΔE(UMP2) = 28.7 kJ mol^{-1} ν = 517 cm^{-1}					
C^α	13.4	4.5	11.2	5.1	18.6	21.
H^α	−20.9	0.5	1.9	0.6	−20.3	−18.3
N	0.6	0.0	0.1	0.1	0.7	0.5
H_N	−1.3	−0.5	0.0	−0.5	−1.8	−1.6

[a] Vibrational corrections are added to a ($\alpha = 0°$) values multiplied by the ratios between UCCSD[T]/TZP+ and UMP2/HD values in the NH_2CH_2 radical (see Table 2).

Coming to the glycine radical, we recall that, among low frequency vibrations, only those involving inversion at the radical center have a significant effect on EPR parameters. The a″ normal mode that corresponds to radical inversion (wag C^α) is well separated and has a sufficiently low harmonic frequency (457 cm^{-1}) to require an anharmonic treatment. On these grounds, the potential energy governing the inversion motion and the corresponding evolution of hyperfine coupling constants have been computed at the UMP2/HD level (see Figure 5). This level of sophistication represents, in our opinion, the best compromise between reliability and computational times for molecules of this dimension. Furthermore, the above results on NH_2CH_2 allow a rescaling of the UMP2/HD results to improve agreement with experiment. As previously reported for the methyl radical, inclusion of anharmonicity increases the inversion frequency (see Table 3). It is quite apparent that the hyperfine coupling constants of H^α and, especially C^α are strongly influenced by out-of-plane motion at the radical center. For C^α the coupling increases with out-of-plane displacement of H^α, and this is clearly related to a strong change in hybridization. At the same time the hfs of H^α increases more smoothly in absolute value. The hsf of other atoms are essentially unsensitive to out of plane motion.

Two sets of experimental EPR parameters can be found in the literature for the GlyR residue. The first one[6] concerns the free radical obtained in pyruvate formate−lyase (PFL) and located on glycine-734. Measurements were performed at 255 K on a aqueous solutions of the radical enzyme. A multiplet structure was observed, where a readily solvent exchangeable proton was responsible for the dominating doublet splitting (a_{iso} = 15 G), whereas the partially resolved sub-doublet splitting

Table 4. Experimental Isotropic Hyperfine Splittings (Gauss) Are Compared with UMP2/HD Results for Different Conformations of F−GlyR−NHCH$_3$. The Computed Energy Differences (ΔE in kJ/mol) between Different Structures Are Also Given

	experimental			theoretical[a,b]					
	ref 6	ref 7	ref 3,5	$\langle\Delta a\rangle$[c]	C_5[d]	α'[e]	α helix[f]	bridge[g]	C_7[h]
				5.0	15.2	16.6	24.7	25.7	30.5
a_C	16−21		24		(23.6)	(25.3)	(35.2)	(35.4)	(42.2)
				3.4	−20.4	−22.5	−24.2	−28.2	−28.9
$a_{H\alpha}$	15	14	17		(−15.1)	(−17.0)	(−18.5)	(−22.1)	(−22.8)
				0.3	−5.1	−3.8	19.6	27.5	28.2
$a_{H\beta}$(NH)	6 or 4.5		1−2		(−4.1)	(−3.0)	(17.3)	(24.1)	(24.7)
$a_{H\gamma}$(CH$_3$)	4.5 or 6		3−5		3.7	2.2	2.9	3.4	1.4
ΔE					0.0	52.7	72.0	92.9	79.9

[a] Bond lengths and valence angles are fixed to the values optimized for the C_5 conformation of F−GlyR−NH$_2$ at the UHF/HD level; the NC and CH distances of the terminal methyl group are frozen to 1.44 and 1.09 Å, respectively, the HCN angles to tetrahedral values, and one of the CH bonds eclipses the adjacent NH bond. [b] For each conformation are given the computed hfs and (in parentheses) the value scaled by the ratio between UCCSD[T]/TZP$^+$ and UMP2/HD results for NH_2CH_2 (see Table 2) and corrected for vibrational effects. [c] Vibrational correction computed for the F−GlyR−NH$_2$ model. [d] $\phi = 180°$, $\psi = 180°$. [e] $\phi = 172°$, $\psi = -10°$. [f] $\phi = 60°$. [g] $\psi = 30°$. [g] $\phi = 90°$, $\psi = 0°$. [h] $\phi = 90°$, $\psi = -60°$.

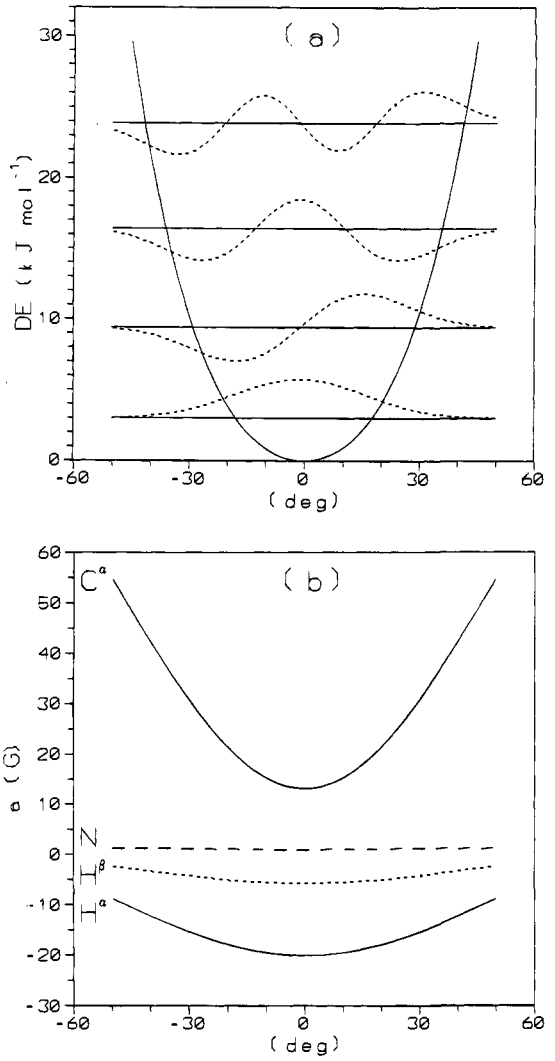

Figure 5. (a) Potential energy and lower vibrational wave functions (normalized to 10) for out-plane motion of H^α computed at the MP2/HD level. (b) Dependence of isotropic hfs on the out of plane angle θ computed at the MP2/HD level. All the results refer to the C_5 conformation of F−GlyR−NH$_2$.

comes from two nonexchangeable protons at about 6 and 4.5 G. The large hfs of 15 G was attributed to the H^α atom, whereas the additional hfs remained unassigned, although they have been tentatively attributed to H^β (NH) and/or H^γ protons located on adjacent amino acid residues. From $^{12}C/^{13}C$ replacements it was proven that the radical is centered at the C^α of the glycine-734 residue. The separation of 49 G between the two distinct features of the EPR spectrum of the isotopically substituted enzyme was assigned to the parallel component of the anisotropic tensor of C^α. From this result, and assuming that the perpendicular component of the anisotropic tensor would be to small to be resolvable, the isotopic hfs of $^{13}C^\alpha$ should lie in the range from 16 to 21 G. The second EPR spectrum attributed to a GlyR residue is obtained at 77 K from a free radical observed in the active anaerobic ribonucleotide reductase (RNR) of Escherichia coli.[7] From previous experimental evidence,[6] it appears that the free radical is localized on the glycine-681 residue of the peptidic chain. After anaerobic activation and transfer of the enzyme solution to an anaerobic EPR tube, a doublet splitting centered at $g = 2.0023$ was observed, with a hfs of 14 G. Unlike the EPR spectrum reported for the glycine-734 radical of PFL,[6] no other hyperfine splittings were observed, and, when the activation step was done in D_2O, an identical doublet was observed. In this case, the signal has a bandwidth of about 7 G, so that the small interactions with other nuclei could not be observed.

The model we have used for the conformational study does not contain appropriate γ hydrogens. In order to investigate the origin of the second hydrogen hfs observed[6]in glycine-734, we have considered a larger model, methylated at the N-terminus. A number of typical conformations have been investigated using the bond lengths and valence angles optimized for the C_5 conformation of F−GlyR−NH$_2$ and the corresponding vibrational corrections to hyperfine splittings. The results of Table 4 eliminate three possible conformations, namely, C_7 ($\phi = 90°$, $\psi = -60°$), bridge ($\phi = 90°$, $\psi = 0°$), and α-helix ($\phi = 60°$, $\gamma = 30°$), and show a remarkable agreement between each of the planar conformations and experimental results. It has, in particular, confirmed the assignment of couplings in the region of 5−6 G to β protons linked to nitrogen and to γ protons of the residue immediately following the glycine radical. A univocal choice between C_5 ($\phi = 180°$, $\psi = 180°$) and α' ($\phi = 170°$, $\psi = -20°$) structures cannot be performed on the basis of hyperfine splittings. Taking, however, into account the significant energy difference between the two conformers, we suggest that the glycine radical residue retains a fully extended conformation also when engaged in peptidic chains, the more so as planar or nearly planar residues are not stabilized by interresidue hydrogen bonds or other long-range interactions.[10]

We have also computed the anisotropic hfs of all atoms at the UHF/HD level. The computed dipolar part of the hyperfine tensor of C^α has a component perpendicular to the moelcular plane of 48 G, and two nearly equal in-plane components of −24 G. Although the values are probably overestimated, they confirm that $A_{||}$ is lower than the experimental resolution of about 7 G.

Conclusions

The present study offers some hints toward the elucidation of the conformational behavior and the EPR parameters of the carbon centered radical derived from the simplest amino acid residue. Our results indicate that only planar or nearly planar conformations are energetically accessible due to effective π-electron delocalization. The hyperfine couplings computed for these conformations are in remarkable agreement with experimental data. This suggests that long-range interactions, even if present, do not alter the intrinsic conformational preferences of this residue. Although further investigations are needed to better elucidate the relevance of long-range interactions in more general terms, the internal consistency of our approach is remarkable and offers considerable promise for the study of EPR characteristics of large systems.

JA941525S